Ruthenium Promotion of Co/Al$_2$O$_3$ Fischer–Tropsch Catalysts

Andreas Kogelbauer,[1] James G. Goodwin, Jr.,[2] and Rachid Oukaci

Department of Chemical and Petroleum Engineering, University of Pittsburgh, Pittsburgh, Pennsylvania 15261

The effect of Ru addition upon catalyst characteristics and performance in Fischer–Tropsch synthesis was investigated using a series of differently prepared, Ru-promoted Co/Al$_2$O$_3$ catalysts. Ru promotion facilitated reduction of Co/Al$_2$O$_3$ leading to catalysts with higher reducibilities. Parallel to this effect, the number of reduced metal atoms exposed on the surface increased for the Ru-promoted catalysts. Ru-promoted catalysts showed an increase in CO hydrogenation activity; however, constant turnover frequencies for promoted and unpromoted catalysts suggest that the increase in the number of metal surface atoms caused the activity enhancement. Isotopic transient kinetic analysis of CO hydrogenation under methanation conditions gave identical results. Catalysts prepared by a co impregnation technique, avoiding chloride salts, appear to be optimal for the production of high-molecular-weight hydrocarbons.

© 1996 Academic Press, Inc.

INTRODUCTION

The conversion of coal and natural gas to fuels and petrochemicals represents one future alternative to the use of limited resources such as crude oil. Although successfully carried out in the 1940s, the Fischer–Tropsch (F–T) synthesis has gained renewed industrial attention due to its potential for such applications. Cobalt-based catalysts are highly attractive for F–T synthesis due to their high activity, selectivity for linear hydrocarbons, low activity for the competing water–gas shift reaction, and lower price compared to noble metals (1). Besides Co as main component, formulations for potential industrial Co F–T catalysts found in the patent literature typically contain a noble metal, oxide promoters, and various supports (2–5).

The noble metal promoter has been suggested to have a number of different ways of affecting catalyst performance. It has been proposed that it acts as a source of hydrogen spillover (1), that it increases the reducibility of Co (6), that it preserves activity by preventing the buildup of carbonaceous deposits (7), that it exhibits cluster and ligand effects (8), and that it provides a combination of enhanced Co reducibility and dispersion (9). It has even been reported that

the addition of a second metal component may have no or a detrimental effect on CO hydrogenation activity (10).

A comprehensive evaluation in our laboratories of various catalyst formulations for the production of highly active and selective Co based F–T catalysts (11, 12) has indicated that alumina-supported Co catalysts are among the most promising candidates. Due to the inconsistencies in the literature regarding the effect of noble metal addition, a careful study of Ru promotion of Co/Al$_2$O$_3$ catalysts was carried out. The main objective of this study was to determine the way in which Ru promotion of Co/Al$_2$O$_3$ catalysts occurs and, secondly, to determine if and in what way differences in catalyst preparation influence catalyst performance.

EXPERIMENTAL

Catalysts

All catalysts used in this study were prepared by aqueous incipient wetness impregnation. The γ-alumina support (VISTA-B) was calcined in air at 500°C for 10 h and presieved to 0–400 mesh prior to impregnation. The surface area and pore volume of the support, as determined by N$_2$ physisorption at −196°C, were 240 m^2/g and 0.49 cm^3/g, respectively. Cobalt nitrate hexahydrate (Kodak, ACS Grade), ruthenium nitrosyl nitrate (Johnson Matthey, 26.82% Ru), and ruthenium chloride (Johnson Matthey) were used. The incipient wetness impregnation was carried out in a single step followed by drying (115°C for 5 h) and calcination (300°C for 2 h). Some catalysts, however, were prepared by sequential impregnation of Co and Ru with intermediate drying, calcination, or reduction. All noble metal promoted catalysts contained 20 wt% Co and 0.5 wt% Ru (except CoRu[2]/Al contained 2 wt% Ru). The various catalysts used in this study and their preparation procedures are given in Table 1. In order to assess possible modifications of the catalyst caused by sequential aqueous impregnation, a Co catalyst was prepared by impregnating the calcined base Co/Al catalyst with deionized water. Characterization of this catalyst ([w]/Co/Al) did not show any discernible changes induced in the catalyst as a consequence of water impregnation solely. For clarification purposes on how chloride addition affects catalyst

TABLE 1

Al$_2$O$_3$-Supported Co–Ru F–T Catalysts Studied

Catalyst[a]	Impregnation I	Treatment[b]	Impregnation II	Treatment[b]
Co/Al	Co[c]	d	—	c/r/p
[w]/Co/Al	Co[c]	d/c	H$_2$O	c/r/p
CoRu/Al	Co[c], Ru[d]	d	—	c/r/p
CoRu[2]/Al	Co[c], Ru[d]	d	—	c/r/p
[Cl]/CoRu/Al	Co[c], Ru[d]	d	HCl	c/r/p
CoRu[Cl]/Al	Co[c], Ru[e]	d	—	c/r/p
Ru/Co[d]/Al	Co[c]	d	Ru[d]	c/r/p
Ru/Co[c]/Al	Co[c]	d/c	Ru[d]	c/r/p
Co/Ru[d]/Al	Ru[d]	d	Co[c]	c/r/p
Co/Ru[r]/Al	Ru[d]	d/r	Co[c]	c/r/p
Co/Ru[c]/Al	Ru[d]	d/c	Co[c]	c/r/p

[a] Al; Al$_2$O$_3$. M$_2$/M$_1$/Al; sequentially impregnated catalysts with M$_1$ first, M$_2$ second impregnation. M$_1$M$_2$/Al; coimpregnated catalysts. [x]: w, H$_2$O; 2, 2 wt% Ru; Cl, chloride; d, dried; c, calcined; r, reduced.

[b] d, dried (static, 115°C, 5 h); c, calcined (static, 300°C, 2 h); r, reduced (flowing H$_2$, 350°C, 10 h); p, passivated (flowing 2% O$_2$ in He, 25°C, 2 h).

[c] Co(NO$_3$)$_2$ · 6H$_2$O.

[d] Ru(NO)(NO$_3$)$_3$.

[e] RuCl$_3$.

performance, [Cl]/CoRu/Al was prepared by incipient wetness impregnation of CoRu/Al after drying (but before calcination) with an aqueous solution of HCl containing equivalent amounts of Cl$^-$ as expected for the catalyst prepared with ruthenium chloride (CoRu[Cl]/Al).

Prior to reaction or characterization, each catalyst was subjected to the same pretreatment cycle consisting of calcination, reduction, passivation, and, if necessary, *in situ* reduction. Calcination was carried out statically in a muffle furnace by raising the temperature in 50°C steps to 300°C and maintaining it for 2 h. Reduction was carried out in flowing H$_2$ (50 cc/min) for 10 h after heating to 350°C at 1°C/min. The catalysts were subsequently passivated in flowing 2% O$_2$/He at ambient temperature for 2 h.

Catalyst Characterization

X-ray measurements were performed on a Philips X'pert System X-ray diffractometer with monochromatized Cu $K\alpha$ radiation in order to identify the Co oxide phases present as well as to estimate the average Co particle size. The spectra were scanned at a rate of 2.4°/min (in 2θ). Since, in most cases, only the diffraction patterns of Co oxide phases could be observed, even when the catalyst was reduced and passivated, the catalysts were used in their calcined form to estimate the Co particle size. The average size of the Co$_3$O$_4$ crystallites in the calcined catalysts was determined from the line width of the most intense reflection applying the Scherrer equation (13).

Dispersion and particle size of the reduced catalysts were determined by H$_2$ chemisorption using a pyrex vacuum system following the procedure described by Reuel and Bartholomew (14). The catalysts were reduced in flowing H$_2$ (50 cc/min) at 350°C for 10 h following heating at 1°C/min. After reduction, the cell was evacuated below 10^{-6} mm Hg. H$_2$ was initially adsorbed at 100°C for 5 h while the total adsorption isotherm was recorded at ambient temperature. The number of exposed metal atoms on the surface was calculated by extrapolating the total adsorption isotherm to zero pressure, assuming a coverage of one H atom per Co^0 atom exposed on the surface.

For determination of the reduction behavior and the reducibility of the catalysts, TPR experiments were carried out in an automated Altamira Instruments AMI-1 system. The calcined catalyst was initially heated under Ar flow at 120°C for 30 min to remove water. A 5% H$_2$/Ar gas mixture (Matheson) was used as the reducing gas with a flow rate of 30 cm^3/min. The catalyst was heated to 900°C at a rate of 5°C/min. The effluent gas was sent through a cooling trap (at less than −50°C) to condense and collect the water generated by the reduction process. The amount of H$_2$ consumed by the catalyst was detected using a thermal conductivity detector (TCD) and recorded as a function of temperature. The reducibility of calcined Co catalysts up to 900°C as well as the amount of unreduced Co after pre-reduction in 1 atm of H$_2$ (50 cc/min) at 350°C for 10 h was determined from these measurements. The extent of reduction after H$_2$ treatment at 350°C for 10 h was also determined by measuring the amount of O$_2$ consumed for reoxidation of the prereduced catalyst using pulse reaction (15). Pulse oxidation was carried out at 400°C using pulses of UHP oxygen of defined volume (50 μl) and monitoring the reactor effluent with the TCD. The extent of reduction was determined as the fraction of reduced cobalt oxidized during the pulse oxidation, assuming Co$_3$O$_4$ to be formed.

Fischer–Tropsch Synthesis

F–T synthesis was carried out at 220°C, 1 atm, and a H$_2$/CO feed ratio of 2 in a fixed bed flow reactor under differential conditions. Thermocouples at the top and at the bottom of the catalyst bed assured precise temperature control during pretreatment and reaction. Typically, 0.2–0.4 g of pretreated catalyst were re-reduced *in situ* in flowing H$_2$ (50 cc/min) at 350°C for 10 h prior to reaction. In order to avoid exotherms and hot spots that lead to rapid catalyst deactivation, the reaction was initiated in a controlled manner by gradually increasing the reactant concentrations over a period of 2 h. After the start-up, samples were taken in 2-h intervals and analyzed by GC. Steady state was reached after 24 h in all cases.

Steady-State Isotopic Transient Kinetic Analysis (SSITKA) of Methanation

Isotopic transient kinetic analysis was carried out in a flow microreactor system (16) under methanation condi-

tions at a temperature of 220°C, a total pressure of 1.8 atm, a CO feed concentration of 2%, a H_2/CO ratio of 10 (He being the balance), and a total flow of 100 cm^3/min (GHSV of ca. 600,000 h^{-1}). These conditions assured avoidance of heat and mass transfer limitations. Prior to reaction, the catalyst (15–30 mg) was reduced *in situ* under flowing H_2 (50 cc/min) at 350°C for 10 h. The transient response of the reactor effluent was monitored after switching from ^{12}CO to ^{13}CO using an on-line mass spectrometer interfaced with a computer. A trace amount of Ar in the ^{12}CO was used to determine the gas phase holdup. The residence times of methane and CO as well as the surface concentrations of intermediates at steady-state were determined for the promoted and the unpromoted catalysts.

RESULTS

Figure 1 shows the results of the TPR measurements for the base cobalt catalyst (Co/Al) and the ruthenium-promoted cobalt catalyst CoRu/Al. The cobalt catalyst exhibited two peaks at 230 and 320°C and a broad reduction feature between 400 and 800°C. The ruthenium-promoted catalyst exhibited two reduction peaks at 230° and 440°C, respectively. The intensity of the low temperature reduction peak at 230°C of Co/Al was greatly diminished by prolonged calcination (see Fig. 2). Mass spectrometer analysis of the gas phase confirmed that the cobalt species corresponding to the low temperature reduction peak was incompletely decomposed $Co(NO_3)_2$. On Ru-promoted catalysts, however, this peak was not solely due to the reduction of $Co(NO_3)_2$, as indicated by the remaining peak in the TPR trace of CoRu/Al in Fig. 3 after 14 h of calcination at 300°C. Only a small fraction of the nitrate (approximately 5–10%)
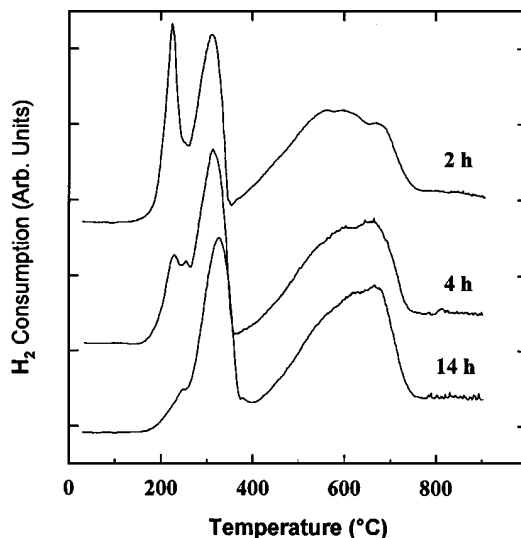
FIG. 2. Effect of calcination time at 300°C upon TPR of Co/Al.

was determined to be present after 2 h of calcination at 300°C. After complete decomposition of the $Co(NO_3)_2$, both the promoted and unpromoted Co/Al_2O_3 catalysts reduced in two steps (Fig. 3), but the low temperature reduction peaks for the Ru-promoted catalyst were about 100°C lower in temperature. In addition, the broad high temperature reduction feature around 600°C, associated with Co species which were extremely difficult to reduce, was replaced by a peak at ca. 450°C in the Ru-promoted Co catalyst. All Ru-promoted catalysts exhibited comparable reduction patterns, as is demonstrated in Fig. 4; however, a reduction at somewhat lower temperature was observed with CoRu[2]/Al.
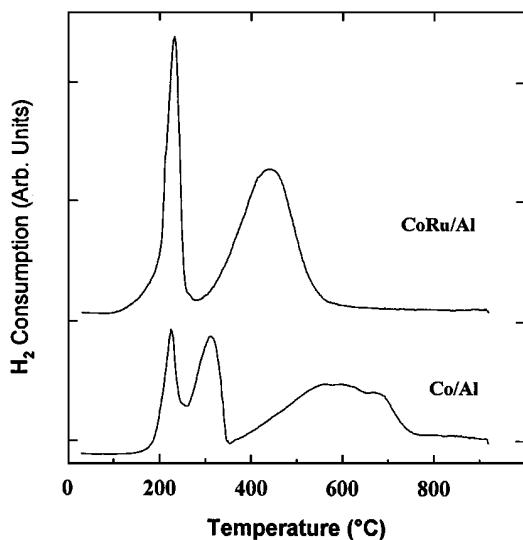
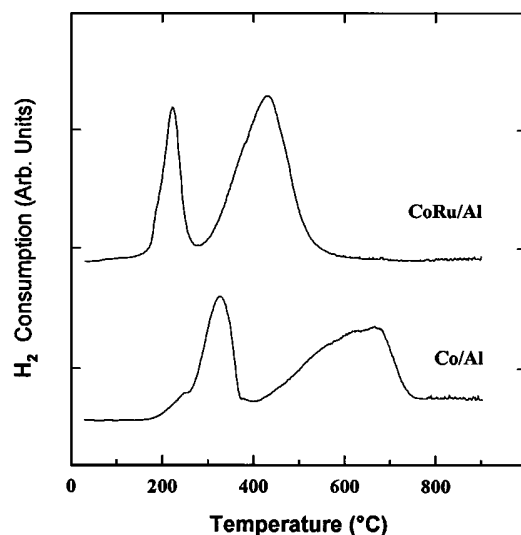**FIG. 1.** TPR of Co/Al and CoRu/Al after calcination at 300°C for 2 h.

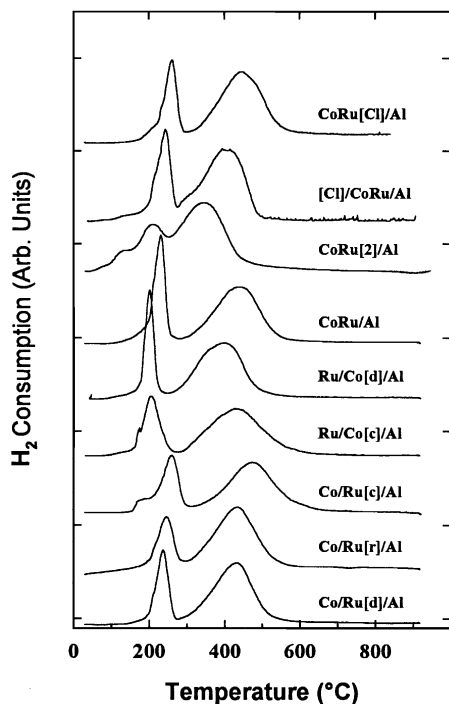**FIG. 3.** TPR of Co/Al and CoRu/Al after calcination at 300°C for 14 h.

FIG. 4. TPR of the differently prepared, Ru-promoted Co/Al$_2$O$_3$ catalysts after calcination at 300°C for 2 h.

A summary of the TPR characterization results for all the catalysts studied is given in Table 2. The reducibility up to 900°C was between >85% for all the calcined catalysts and slightly higher (>95%) for those Ru-promoted catalysts prepared by co-impregnation (CoRu/Al, CoRu[2]/Al, CoRu[Cl]/Al). The extent of reduction *after standard reduction treatment* in 1 atm of flowing H$_2$ (50 cc/min) at 350°C for 10 h, however, was significantly smaller for Co/Al (ca. 60%) compared to the Ru-promoted catalysts which exhibited reducibilities between 85 and 100%. Ru/Co[c]/Al showed the smallest extent of reduction among the Ru-promoted catalysts prepared by sequential impregnation. It should be noted that the values for the extent of reduction as determined by TPR of the reduced catalyst and by pulse oxidation agreed very well.

The data in Table 2 show that addition of ruthenium not only increased the extent of reduction but compared to the unpromoted catalyst also resulted in approximately three times the number of exposed cobalt atoms at the surface of all Ru-promoted catalysts as measured by chemisorption of H$_2$. In parallel, the average Co metal particle size for the ruthenium-promoted catalysts (determined from H$_2$ chemisorption and the amount of reduced Co present) decreased and was roughly half of that of the unpromoted Co/Al catalyst.

The determination of the particle size of the calcined catalysts by XRD indicates comparable sizes of around 15 ± 4 nm for all catalysts prior to reduction. All catalysts showed exclusively diffraction patterns of Co$_3$O$_4$ and γ-alumina with the exception of Ru/Co[c]/Al, which also showed reflections due to RuO$_2$.

The rate of F–T synthesis at 220°C increased by a factor of ca. 3 for CoRu/Al relative to Co/Al (see Table 3). As can be seen from the similar values of the chain growth probability α (see also Fig. 5) and the CH$_4$ selectivity, there was only a minute influence of Ru on the product distribution. Minor deviations from this behavior were observed for the catalysts prepared by addition of HCl ([Cl]/CoRu/Al) or the use of ruthenium chloride (CoRu[Cl]/Al), as indicated by the higher methane selectivity together with a lower chain growth probability. The differences were nevertheless very small. The catalysts prepared sequentially from the Co/Al$_2$O$_3$ precursor (Ru/Co[d]/Al, Ru/Co[c]/Al) showed similar selectivities (CH$_4$, α) but lower rates. Calcination of the precursor produced a catalyst (Ru/Co[c]/Al) with the lowest rate compared to all the Ru-promoted catalysts in this study. The variation in rates observed at steady-state was comparable to that for "initial" rates. Figure 6 shows the change in the F–T synthesis rate with time-on-stream for a number of the catalysts. In all cases a decrease by ca. 25% of the original rate (measured after 2 h on-stream following the controlled initiation of the reaction) was observed.

The addition of ruthenium increased only slightly the specific rate expressed as turnover frequency (TOF, based on the number of reduced surface cobalt atoms measured from H$_2$ chemisorption). All ruthenium-promoted catalysts exhibited comparable TOFs. Considering the variation in these values (0.018–0.025) the differences between unpromoted and promoted catalysts appear rather small.

The SSITKA results for CO hydrogenation on Co/Al and CoRu/Al are compiled in Table 4. From the measured average surface intermediate residence times, τ, values for the intrinsic rate constant k (for CH$_4$), the surface abundances N_i, and the surface coverages Θ_i under reaction conditions were calculated (17). Figure 7 shows a representative example of transient responses obtained for all catalysts. The rates of reaction (footnote A to Table 4) agree very well with those reported in Table 3, indicating that despite the different reaction conditions (partial pressures, GHSV) and the high methane selectivity, CO hydrogenation under methanation conditions reflects well the catalyst behavior under low conversion F–T conditions. The intrinsic pseudo-first-order rate constant, estimated by $1/\tau_{CH_4}$ (where τ_{CH_4} is the average residence time of CH$_4$ intermediates on the surface), was essentially the same for both the promoted and the unpromoted catalyst, whereas the number of CH$_4$ intermediates was approximately four times higher for the Ru-promoted catalyst. Similarly, the abundance of CO on the surface was higher by the same factor. Thus, the fractional surface coverages of CO and CH$_4$ were approximately the same for the promoted and unpromoted catalysts.

TABLE 2

Characterization Results for Co–Ru/Al$_2$O$_3$ Catalysts

Catalyst	H$_2$-TPR (reducibility up to 900°C, %)			Pulse Oxidation (% reoxidized after reduction at 350°C)	H$_2$ Chemisorption		
	After calcination at 300°C	After[a] reduction at 350°C	Difference[b]		Amount[c] (μ mol H/g cat)	Overall dispersion[d] (%)	d_p[e] (nm)
Co/Al	85	25	60	58	95	2.8	21
CoRu/Al	97	3	94	101[f]	285	8.4	12
CoRu[2]/Al	98	0	98	—	333	9.3	9
[Cl]/CoRu/Al	95	—	<95	103[f]	—	—	—
CoRu[Cl]/Al	98	—	<98	—	264	7.8	13
Ru/Co[d]/Al	91	2	89	88	247	7.3	13
Ru/Co[c]/Al	92	8	84	85	258	7.6	11
Co/Ru[d]/Al	88	—	<88	86	308	9.1	10
Co/Ru[r]/Al	86	—	<86	86	268	7.9	11
Co/Ru[c]/Al	88	—	<88	82	231	6.8	13

[a] Percentage of metal still reducible after *in situ* reduction of catalyst under H$_2$ at 350°C for 10 h.

[b] Represents percentage of metal reduced after standard reduction procedure (ramp 1°C/min to 350°C, hold at 350°C for 10 h).

[c] Assuming a coverage of one H atom per exposed Co^0 atom on the surface.

[d] Dispersion related to total number of cobalt atoms present.

[e] Particle size is based upon reduced cobalt ($d_p = 5\rho/S_{Co}$, where S_{Co} is the surface area of red. Co/g of red. Co).

[f] Overestimated most probably due to inaccuracies in the determination of the baseline during initial O$_2$ pulses.

DISCUSSION

Bulk Co$_3$O$_4$ is known to reduce in two steps from Co$_3$O$_4$ to CoO and then to Co metal (18). Two separate reduction peaks are not always observed for the bulk oxide in TPR (19–21); however, it has been claimed that interactions with support materials such as silica or alumina may lead to a more distinct splitting of the two reduction peaks (14, 21). Two reduction peaks were observed for Co/Al, having maxima at 320°C and ca. 600°C. If the high temperature reduction peak were associated with the reduction of CoO to Co^0, one would expect CO^{2+} to be present almost exclusively after standard reduction at 350°C resulting in an inactive catalyst for CO hydrogenation. However, standard reduction before CO hydrogenation was carried out in 1 atm of flowing H$_2$ and was able to produce an active catalyst, indicat-

TABLE 3

Steady-State CO Hydrogenation Results for the Co–Ru/Al$_2$O$_3$ Catalysts[a]

Catalyst	Rate (g CH$_2$/g cat./h)	TOF[b] (s^{-1})	CH$_4$ (%)	α
Co/Al	0.077	0.015	29.2	0.62
CoRu/Al	0.290	0.020	30.0	0.62
CoRu[2]/Al	0.310	0.018	29.0	0.64
[Cl]/CoRu/Al	0.320	—	33.5	0.57
CoRu[Cl]/Al	0.342	0.025	31.1	0.57
Ru/Co[d]/Al	0.254	0.021	29.7	0.61
Ru/Co[c]/Al	0.227	0.018	30.0	0.60
Co/Ru[d]/Al	0.328	0.021	32.4	0.58
Co/Ru[r]/Al	0.311	0.023	31.7	0.58
Co/Ru[c]/Al	0.287	0.025	30.4	0.60

[a] Accuracy of kinetic, measurements: rates, ±5%; α, ± 3%; selectivities, ± 3%.

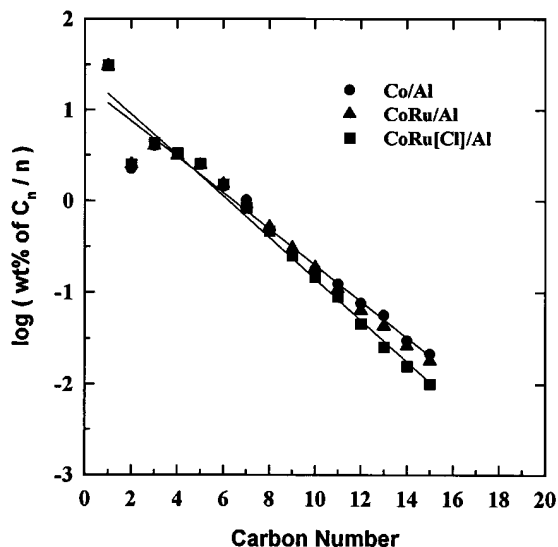[b] based upon H$_2$ chemisorption (CO molecules/site/s).

FIG. 5. Anderson–Schulz–Flory distribution of F–T synthesis products for Co/Al and CoRu/Al (220°C, 1 atm, H$_2$/CO = 2).
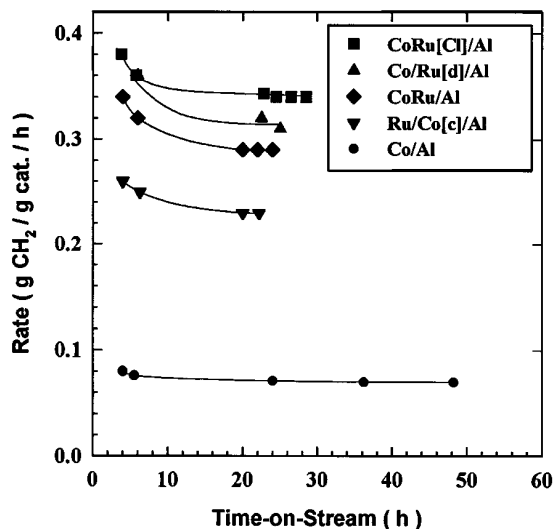
FIG. 6. Rates of F–T synthesis at 220°C, 1 atm, and $H_2/CO = 2$ vs time-on-stream for selected catalysts.

FIG. 7. Transient response after switch from ^{12}CO to ^{13}CO during CO hydrogenation on Co/Al at 220°C, 1.8 atm, and $H_2/CO = 10$.

ing the presence of Co metal. TPR of Co/Al *pre-reduced at 350°C* showed only one reduction peak at about 600°C with ca. 40% of Co still unreduced. This confirms that the catalyst's F–T activity originates from cobalt reduced around 350°C in pure H_2. While the two TPR peaks seen may represent a separation of the two reduction steps during TPR in a 5% H_2/Ar mixture using a fast temperature rise of 5°C/min, they could also represent two different states of Co_3O_4 with different ease of reduction. For instance, one might suggest that the low temperature peak may be due to easily reduced oxides on or near the surface of crystallites (22, 23), whereas the high temperature peak may be due to less easily reduced bulk oxide and/or the presence of strong interactions of the metal oxide with the Al_2O_3 support (19, 24–26). It should be noted that the high temperature peak exhibited a strongly asymmetric form, suggesting the presence of at least two distinct high temperature, reduction peaks which could account for both bulk oxide and Co_3O_4 in strong interaction with the support. Another notable feature of the TPR of Co/Al was the apparent base line shift at high temperature, indicating that reduction was not complete even at
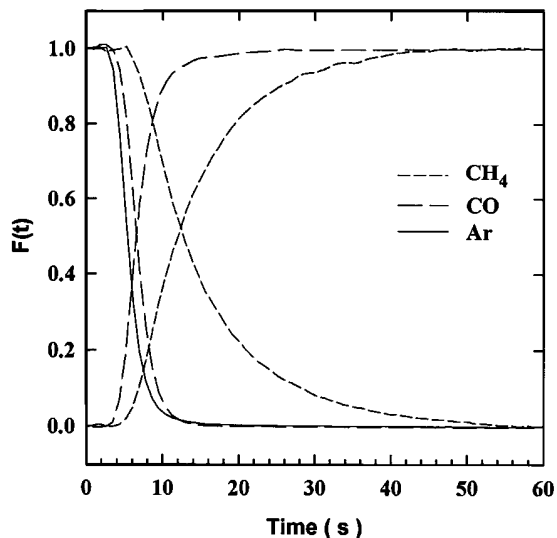
900°C. Co is known to undergo compound formation with alumina during calcination (20, 27, 28), leading to hardly reducible and nonreducible (<900°C) Co aluminates. The incomplete reduction of Co/Al and the reduction of Co at very high temperatures are possibly due to the presence of such Co–Al compounds.

Based on MS analysis of the gas phase, the lowest reduction peak at 230°C which disappeared upon extended calcination was attributed to the presence of incompletely decomposed nitrate after 2 h of calcination (21). TPR of the prereduced catalyst confirmed that this residual nitrate was reduced during standard reduction at 350°C. Since the reduction of Co nitrate is strongly exothermic (21), it may enhance the formation of hardly reducible Co–Al compounds and, as such, contribute to catalyst deterioration. Judging from the constant values of the reducibility after extended calcination times (2–14 h, with complete nitrate removal), the decomposition of the residual nitrate during reduction in the 2-h calcined catalyst did not appear to affect catalyst morphology, perhaps due to the low heating rate of 1°C/min during standard reduction.

TABLE 4

SSITKA Results for the Co–Ru/Al$_2$O$_3$ Catalysts

Catalyst	Rate[a] (μmol/g Co/s)	CH_4 (%)	τ_{CH_4}[b] (s)	τ_{CO}[b] (s)	k_{CH_4} (s^{-1})	N_{CH_4} (μmol/g Co)	N_{CO} (μmol/g Co)	Θ_{CH_4}	Θ_{CO}
Co/Al	7.1	64	10.8	1.1	0.093	52	246	0.11	0.52
CoRu/Al	26.6	68	10.5	2.0	0.095	190	835	0.13	0.59

[a] Values reported correspond to 0.072 and 0.268 g CH_2 (g catalyst)$^{-1}$ h^{-1}, respectively.
[b] Accuracy of residence times: CH_4, ±1 s; CO, ±0.2 s.

The addition of Ru to the Co catalyst made the reduction of the catalyst easier which was concluded from the shift (by about $100°C$) of the maxima in the rate of reduction to lower temperatures. Increasing the amount of Ru to 2 wt% additionally shifted the reduction maxima somewhat to lower temperature. It has been proposed that noble metals activate hydrogen and thereby become a source for hydrogen spillover to Co_3O_4, thus promoting its reduction at a lower temperature (1). This would lead to a higher extent of reduction in the Ru-promoted catalysts after standard reduction treatment compared with Co/Al. The impact of Ru promotion on Co reducibility ($<900°C$), however, is manifested not solely in lower reduction temperatures but also in the approximately complete reduction of Co, compared with only 85% reducibility for Co/Al. This would suggest that Ru either prevents the formation of highly irreducible Co compounds (Co oxide strongly interacting with the Al_2O_3 or Co aluminates) or promotes their reduction if formed. It would be highly speculative at this point to attempt to conclude more for this system. However, based on their study of Pt-promoted Co/Al_2O_3, Schanke et al. (36) have suggested that Pt does not help to reduce Co aluminates. It is likely that the mechanisms of Ru and Pt in promoting Co/Al_2O_3 are similar.

Besides the increased facilitation of Co reduction, Ru-promoted catalysts exhibited also a better dispersion of Co metal than the unpromoted catalyst as indicated by H_2 chemisorption (i.e., more surface exposed Co^0 atoms). Since the average Co metal particle size calculated was based upon both the amount of surface exposed Co metal atoms and the amount of reduced Co, it can be suggested that Ru acted to increase the physical dispersion of the reduced cobalt. Since there was an increase in H_2 chemisorption and reducibility even when Ru was added to a precalcined Co catalyst and it is unlikely that Ru acted to break apart Co oxide particles already extant during reduction, one can suggest that Ru possibly aids in reducing small Co oxide patches strongly interacting with the support to produce additional small particles or raft-like structures of reduced Co metal. The presence of these additional small metal particles would greatly decrease the average Co metal particle size determined using a combination of H_2 chemisorption and TPR.

The amount of Ru used as promoter in excess of 0.5 wt% had only a slight effect. Addition of 2 wt% instead of 0.5 wt% Ru resulted in ca. 15% higher H_2 chemisorption. However, it did not result in a significantly increased CO hydrogenation activity.

The importance of the calcination step to achieve highly active Co and Co–Ru catalysts has been previously recognized (29). This has been attributed to the formation of well mixed Co-Ru phases by migration of mobile Ru oxide species (7).

The increase in reducibility and in the number of surface metal atoms was also reflected in the catalytic performance of the Ru-promoted catalysts. Since it has been shown that particle size effects are not present in CO hydrogenation over Co catalysts (30, 31), the practically constant TOF values for CO hydrogenation suggest that the increase in activity is predominantly caused by an increase in number of sites rather than by an electronic effect. When particle size effects are seen, they have been suggested to be due to incompletely reduced catalysts or the presence of Co aluminates (32).

Iglesia et al. (7) reported that Ru promotion of silica- and titania-supported Co catalysts caused a synergistic effect in which the specific rates of CO hydrogenation expressed as TOFs based on H_2 chemisorption increased upon addition of small amounts of Ru. They explained the beneficial action of Ru to be a cleansing effect during CO hydrogenation due to its high hydrogenation ability which prevented the formation of carbon deposits on the catalyst surface. In a report by Shpiro et al. (8), the phrase synergy was used rather ambiguously to describe the increase in CO conversion for Co–Ru/Al_2O_3 catalysts compared to Co/Al_2O_3. Although an increase in reducibility after Ru promotion was reported (8), the lack of chemisorption data makes a comparison based on TOF impossible.

Despite the fact that the TOFs reported in Table 3 for unpromoted and promoted catalysts can be considered essentially the same, a more thorough investigation concerning the possible presence of effects other than increased Co^0 dispersion was deemed necessary. Since steady-state TOF is a product of intrinsic rate constant and surface coverage (33, 34), SSITKA was chosen to allow differentiation of the contribution of both quantities to the TOF. This enabled us to assess if an increase in the intrinsic rate was due only to an increase in the number of surface sites (as reflected by the number of surface intermediates) or also included an increase in intermediate/site activity. The intrinsic rate constant for methanation was determined to be the same for both promoted and unpromoted catalysts, whereas the number of intermediates increased by the same factor as the overall rate of CO hydrogenation. Given the corresponding increase in H_2 chemisorption, this suggests that Ru promotion increases the reaction by increasing the Co metal dispersion, thereby increasing the number of reaction sites. These additional sites appear to be identical to those present in the absence of Ru. Vada et al. (9) reached similar conclusions for the effect of Re and Pt promotion of alumina-supported Co catalysts. The similar CH_4 selectivities and α values during F–T synthesis also lead to the conclusion that Co dominates the catalytic behavior of Co–Ru/Al_2O_3 catalysts for low loadings of Ru. This may be better understood if one considers the crystallite surface to be enriched in Co (8). Based on XPS data of Ru-impregnated

Co foils, however, Iglesia *et al.* (7) concluded that for TiO$_2$-supported Co–Ru catalysts the crystallite surface was enriched in Ru. Although we cannot completely exclude a synergism as suggested by these authors (7), the similar TOFs, coverage of reactive species under reaction conditions, product selectivities, and the deactivation behaviors of the Ru-promoted and unpromoted catalysts makes this possibility rather improbable for Al$_2$O$_3$-supported catalysts.

Among the different preparation techniques, only small differences were observed. For the coimpregnated CoRu/Al catalysts, Ru promotion led to higher reducibility and higher Co^0 dispersion of the catalysts. The reduction patterns during TPD suggest identical action of Ru in sequentially impregnated, and coimpregnated catalysts. Nevertheless, the efficiency of Ru promotion, appraised by the rate of CO hydrogenation, was worst for Ru/Co[c]/Al, the catalyst that was prepared by Ru impregnation of the calcined Co/Al$_2$O$_3$ precursor. The TOF, however, remained constant for this catalyst, indicating that the lower rate is explicitly due to a smaller number of Co reaction sites. There was a somewhat smaller decrease in the rate of CO hydrogenation if the catalyst was prepared by sequential impregnation of Ru onto the dried Co/Al$_2$O$_3$ precursor.

For the catalysts prepared by sequential impregnation of Co on Ru/Al$_2$O$_3$ precursors the CO hydrogenation rates were comparable or somewhat higher than those for the coimpregnated catalysts. Calcination of Ru before Co impregnation yielded the catalyst with the lowest F–T activity in this series. Both the higher temperatures of the maxima in the TPR traces, indicating less efficient promotion of reduction, and the presence of a low temperature shoulder at 200°C for Co/Ru[c]/Al, similar to that for Ru/Al$_2$O$_3$ alone, suggest that intimate mixing of the metal components did not occur completely. This is consistent with the observation of a RuO$_2$ phase in the XRD patterns of the calcined catalyst. Drying Ru only or reducing it gave catalysts with slightly higher activity, but also higher CH$_4$ selectivity and slightly lower chain growth probability.

The nature of the Ru salt was found to have little effect on the Ru-promoted Co catalysts. Contrarily, significant changes in selectivity and activity for CO hydrogenation have been reported to occur for supported Ru catalysts prepared using different Ru salts (35). It was suggested that this may be due to structural rearrangement of the metal surface induced by the initial presence of chloride ions. However, for the CoRu/Al$_2$O$_3$ catalyst the similar reduction patterns during TPR as well as the comparable characterization results suggest a generally similar effect whether Ru chloride or Ru nitrosyl nitrate is used. Although CO hydrogenation rates were higher when Ru chloride was used, this increase may be attributable to increased formation of low molecular hydrocarbons as indicated by increased CH$_4$ selectivities and lower α.

CONCLUSIONS

The addition of small amounts of ruthenium to γ-alumina-supported cobalt catalysts facilitated the reduction of the Co catalyst. This was concluded from the lowering of the reduction temperatures during TPR by approximately 100°C and the essentially complete reduction of the Ru-promoted catalyst (CoRu/Al) at 350°C compared to only a 60% reduction of the unpromoted Co/Al catalyst. In parallel, the amount of metal atoms exposed on the surface determined by H$_2$ chemisorption increased by a factor of 3 upon Ru promotion. The increase in surface exposed metal atoms was paralleled by an equivalent increase in the rate of CO hydrogenation, yielding practically constant turnover frequencies. SSITKA results indicated constant intrinsic activities but an increase in the number of reaction intermediates at constant coverages when a Ru-promoted catalyst was compared to the unpromoted Co catalyst. There was little change in product selectivity. Promotion with more than 0.5 wt% Ru improved the catalyst characteristics only marginally. From these results we conclude that ruthenium acts only as a reduction promoter for Co by increasing the reducibility and dispersion of the cobalt. These results for Ru promotion are compatible with those recently reported for Pt-promoted Co F–T catalysts (36).

Ruthenium appeared to inhibit the formation of highly irreducible Co species (Co oxide strongly interacting with the support or Co aluminates) or to promote their reduction, indicated by the absence of the broad high temperature TPR feature observed with Co/Al$_2$O$_3$ and the greater degree of reduction. Calcination of Ru/Al$_2$O$_3$ or Co/Al$_2$O$_3$ precursors prior to a sequential impregnation of Co or Ru, respectively, impeded the intimate mixing of the metal components. Coimpregnation of the metal salts appeared to produce catalysts slightly more active for CO hydrogenation.

REFERENCES

1. Goodwin, J. G., Jr., *Prep. ACS Div. Petr. Chem.* **36**(1), 156 (1991).
2. Iglesia, E., Soled, S., and Fiato, R. A., U.S. patent 4,794,099 (1988).
3. Beuther, H., Kibby, C. L., Kobylinski, T. P., and Pannell, R. B., U.S. patent 4,413,064 (1983).
4. Post, M. F. M., and Sie, S. T., European Pat. Appl. 0 167 215 A2 (1986).
5. Eri, S., Goodwin, J. G., Jr., Marcelin, G., and Riis, T., U.S. patent 4,880,763 (1989).
6. Takeuchi, K., Matsuzaki, T., Arakawa, H., Hanaoka, T., and Sugi, Y., *Appl. Catal.* **48**, 149 (1989).
7. Iglesia, E., Soled, S. L., Fiato, R. A., and Via, G. H., *J. Catal.* **143**, 345 (1993).

8. Shpiro, E. S., Tkachenko, O. P., Belyatskii, V. N., Rudnyi, Y., Telegina, N. S., Panov, S. Y., Gryaznov, V. M., and Minachev, K. M., *Kinet. Catal.* **31**, 832 (1990).

9. Vada, S., Hoff, A., Adnanes, E., Schanke, D., and Holmen, A., *Topics Catal.* **2**, 155 (1995).

10. Villeger, P., Barrault, J., Barbier, J., Leclercq, G., and Maurel, R., *Bull. Soc. Chim. Fr.* **9–10**, 413 (1979).

11. Oukaci, R., Goodwin, J.G., Jr., Marcelin, G., and Singleton, A., *Prep. ACS Div. Fuel Chem.* **39**(4), 1117 (1994).

12. Oukaci, R., Goodwin, J. G., Jr., Marcelin, G., and Singleton, A., "Proceedings, 11th Annual International Pittsburgh Coal Conference" (S.-H. Chiang, Ed.), Vol. 1, The Univ. of Pittsburgh, Center for Energy Research, Pittsburgh, 1994.

13. Klug, H. P., and Alexander, L. E., *in* "X-ray Diffraction Procedures." Wiley, New York, 1954.

14. Reuel, R. C., and Bartholomew, C. H., *J. Catal.* **85**, 63 (1984).

15. Bartholomew, C. H., and Farrauto, R. J., *J. Catal.* **45**, 14 (1976).

16. Chen, B., and Goodwin, J. G., Jr., *J. Catal.* **154**, 1 (1995).

17. Shannon, S. L., and Goodwin, J. G., Jr., *Chem. Rev.* **95**, 677 (1995).

18. Sexton, B. A., Hughes, A. E., and Turney, T. W., *J. Catal.* **97**, 390 (1986).

19. Arnoldy, P., and Moulijn, J.A., *J. Catal.* **93**, 38 (1985).

20. Wang, W., and Chen, Y., *Appl. Catal.* **77**, 223 (1991).

21. Lapidus, A., Krylova, A., Kazanskii, V., Borovkov, V., Zaitsev, A., Rathousky, J., Zukal, A., and Jancalkova, M., *Appl. Catal.* **73**, 65 (1991).

22. Kogelbauer, A., Weber, J., and Goodwin, J. G., Jr., *Catal. Lett.* **34**, 259 (1995).

23. Koranne, M. M., Goodwin, J. G., Jr., and Marcelin, G., *J. Catal.* **148**, 369 (1994).

24. Delmon, B., and Roman, A., *J. Catal.* **30**, 333 (1973).

25. Houalla, M., Delannay, F., Matsuura, I., and Delmon, B., *J. Chem. Soc. Faraday Trans. I* **76**, 2128 (1980).

26. Mile, B., Stirling, D., Zammitt, M., Lovell, A., and Webb, M., *J. Catal.* **114**, 217 (1988).

27. Chin, R. L., and Hercules, D. M., *J. Phys. Chem.* **86**, 360 (1982).

28. Chung, K. S., and Massoth, F. E., *J. Catal.* **64**, 320 (1980).

29. Beuther, H., Kobylinski, T. P., Kibby, C. L., and Pannell, R. B., U.S. patent 4,585,798 (1986).

30. Ho, S., Houalla, M., and Hercules, D. M., *J. Phys. Chem.* **94**, 6396 (1990).

31. Johnson, B.G., Bartholomew, C. H., and Goodman, D.W., *J. Catal.* **128**, 231 (1991).

32. Rameswaran, M., and Bartholomew, C. H., *J. Catal.* **117**, 218 (1989).

33. Biloen, P., *J. Mol. Catal.* **21**, 17 (1983).

34. Biloen, P., Helle, J. N., van den Berg, F. G. A., and Sachtler, W. M. H., *J. Catal.* **81**, 450 (1983).

35. Iyagba, E. T., Hoost, T. E., Nwalor, J. U., and Goodwin, J. G., Jr., *J. Catal.* **123**, 1 (1990).

36. Schanke, D., Vada, S., Blekkan, E. A., Hilmen, A. M., Hoff, A., and Holmen, A., *J. Catal.* **156**, 85 (1995).